ACS APPLIED MATERIALS & INTERFACES

Research Article

www.acsami.org

Rationally Designed Polyimides for High-Energy Density Capacitor Applications

Rui Ma,[†] Aaron F. Baldwin,[†] Chenchen Wang,[‡] Ido Offenbach,[§] Mukerrem Cakmak,[§] Rampi Ramprasad,[‡] and Gregory A. Sotzing*,[†]

[†]Polymer Program, University of Connecticut, 97 North Eagleville Road, Storrs, Connecticut 06269, United States

[‡]Department of Materials Science and Engineering, University of Connecticut, 97 North Eagleville Road, Storrs, Connecticut 06269, United States

[§]Department of Polymer Engineering, University of Akron, Akron, Ohio 44325, United States

Supporting Information

ABSTRACT: Development of new dielectric materials is of great importance for a wide range of applications for modern electronics and electrical power systems. The state-of-the-art polymer dielectric is a biaxially oriented polypropylene (BOPP) film having a maximal energy density of 5 J/cm^3 and a high breakdown field of 700 MV/m, but with a limited dielectric constant (~2.2) and a reduced breakdown strength above 85 °C. Great effort has been put into exploring other materials to fulfill the demand of continuous miniaturization and improved functionality. In this work, a series of polyimides were investigated as potential polymer materials for this application. Polyimide with high dielectric constants of up to 7.8 that exhibits low dissipation factors (<1%) and high energy density around 15 J/cm^3, which is 3 times that of BOPP, was prepared. Our syntheses were guided by high-throughput density functional theory calculations for rational design in terms of a high dielectric constant and band gap. Correlations of experimental and theoretical results through judicious variations of polyimide structures allowed for a clear demonstration of the relationship between chemical functionalities and dielectric properties.

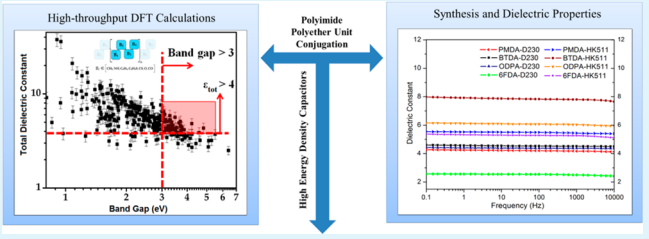

KEYWORDS: *polyimide, dielectric properties, DFT calculations, structure, thermal properties*

1. INTRODUCTION

The demand for developing high-energy density capacitors is based on their indispensable importance in many applications, including hybrid electric vehicles, high-energy lasers, electromagnetic railguns, and proposed systems for inertial confinement fusion (ICF).[1] The energy density of capacitors is governed by their dielectric material, which stores energy electrostatically through polarization.[2] Polymer film capacitors are attractive for these applications because of their low cost, high dielectric strength, low dielectric loss, and graceful failure.[3] The current state-of-the-art polymer dielectric film, biaxially oriented polypropylene (BOPP), has a relatively low dielectric constant and suffers from a low upper operating temperature of 85 °C due to the dramatic increase in electronic conduction at higher temperatures.[4,5] For a linear dielectric, the energy density is proportional to the dielectric constant and the square of the electric field ($U_e = 0.5K\varepsilon_0E^2$, where vacuum permittivity $\varepsilon_0 = 8.85 \times 10^{-12}$ F/m), which is limited by breakdown strength. Therefore, a new dielectric material is required to have higher dielectric constants and better thermal durability while still maintaining low loss and high breakdown strength. Polar polymers are attractive for next-generation dielectrics because orientational polarization can be utilized to achieve a high dielectric constant,[6] proved by polyvinylidene fluoride (PVDF) and copolymers with a dielectric constant of ~10.[7−9] Further exploration of other polar polymers, especially high-temperature polar polymers,[10,11] is essential for understanding the structure−property relationship, to tailor dielectric and thermal properties.

Here, in attempt to identify the polymers with a high dielectric constant and band gap, high-throughput density functional theory (DFT) computations were conducted to perform initial screening. Among the several promising systems, polyimides were chosen to be investigated. Polyimides are widely used in many applications because of their high thermal stability, chemical resistance, electrical characteristics, and dimensional stability. Most research on polyimides has been focused on achieving a low dielectric constant for microelectronics applications.[12−14] For energy storage applications, we are targeting the opposite by seeking structures with a high dielectric constant as well as low dissipation factors.

Polyimides were generated by polymerization of different aromatic dianhydrides and aliphatic diamines (Scheme 1) to increase the polar group density in the backbone and to

Received: April 2, 2014
Accepted: June 9, 2014
Published: June 9, 2014

Scheme 1. Monomers and Syntheses of Polyimides A1−D4

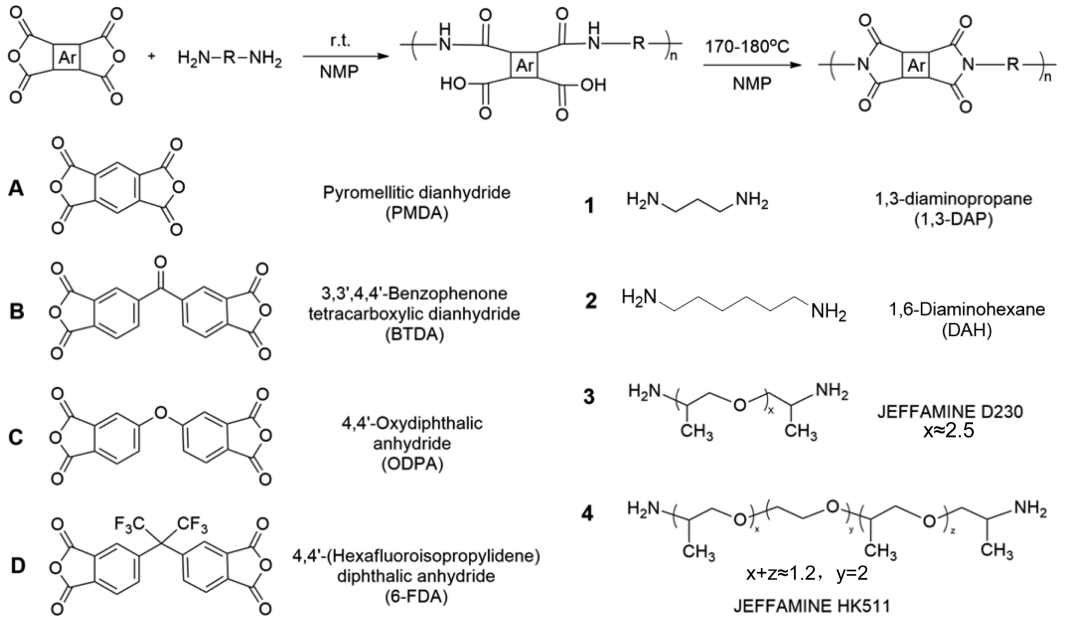

improve solubility. With no catalyst and sole production of water in the synthesis procedure, polyimide with a higher purity minimizes impurity ion migrational loss, which is inherent for PVDF prepared from suspension polymerization. Incorporation of different functional groups such as carbonyl and ether works as additional permanent dipole moments and changes the cross-conjugation length and, hence, alters the delocalization of π-electrons. Dielectric properties, including the dielectric constant and loss at different temperatures and frequencies, band gap, and dc breakdown field, were characterized with a dielectric constant and band gap compared to DFT calculations; however, processing optimization is needed to improve the film quality.

2. EXPERIMENTAL AND CALCULATION METHODOLOGY

2.1. Materials. Pyromellitic dianhydride (PMDA), 3,3′,4,4′-benzophenone tetracarboxylic dianhydride (BTDA), 4,4′-oxidiphthalic anhydride (ODPA), 1,3-diaminopropane (1,3-DAP), 1,6-diaminohexane (DAH), and anhydrous *N*-methyl-2-pyrrolidone (NMP) were purchased from Aldrich Chemical Co., and 4,4′-(hexafluoroisopropylidene) diphthalic anhydride (6-FDA) was purchased from TCI America. Jeffamines D230 and HK511 were provided by Huntsman Corp. Dianhydrides were recrystallized from acetic anhydride before use. Diamines were used as received.

2.2. Instruments. Fourier transform infrared (FTIR) spectra were recorded with a Nicolet Magna 560 FTIR spectrometer (resolution of 0.35 cm^{-1}). Solution ^1H nuclear magnetic resonance (NMR) was performed on a Bruker DMX500 high-resolution digital NMR spectrometer. Gel permeation chromatography (GPC) was conducted using tetrahydrofuran (THF) as the mobile phase and polystyrene standards with the following instruments: Waters 1515 HPLC pump, Waters 717+ autosampler, Waters 2487 dual λ absorbance detector, Varian 380-LC evaporative detector, and two mixed bed Jordi Gel DVB columns. Thermogravimetric analysis (TGA) was performed with a TA Instruments TGA Q500 instrument (heating rate of 10 °C/min under nitrogen), and differential scanning calorimetry (DSC) analysis was performed with a TA Instruments DSC Q-100 instrument with the glass transition and melting point determined from the second heating cycle at a rate of 10 °C/min. Dielectric spectroscopy was conducted using an IMASS time domain dielectric spectrometer. Measurements were made in an air circulating oven at constant temperature by taking frequency scans, with 10 V ac applied. Stainless steel shims purchased from McMaster Carr (diameter of 2 in., thickness of 0.01 in.) were used as the substrates. The UV−vis spectrum for band gap determination was obtained using Varian Cary UV−vis 5000 instrument. The UV−vis spectra were recorded from 200 to 800 nm, and the onset wavelength of absorption, λ_{onset}, was used to determine the band gap (E_g) from Planck's equation: $E_g = (hc)/\lambda_{onset}$.

Breakdown strength measurements were performed using a linear voltage ramp generated by a resistor capacitor (RC) circuit. When the first breakdown event occurs, the power supply is shut off through an interlock input by a silicon-controlled rectifier (SCR) circuit, which uses the breakdown-induced ground-rise voltage capacitively coupled to the gate of an SCR. The breakdown voltage of the sample is read from a peak-holding voltmeter. The sample thickness was determined using a thickness gauge (model LE1000-2, MeasureItAll) as the average of several measurements near the breakdown site.

2.3. Calculation Methodology. DFT calculations were performed using the Vienna *ab initio* simulation package (VASP).[15] The Perdew, Burke, and Ernzerhof functional (PBE), projector-augumented wave (PAW) frozen-core potentials and a cutoff energy of 400 eV for the plane wave expansion of the wave functions were used.[16−18] The optimized geometry was then used to determine the dielectric constant tensor using density functional perturbation theory (DFPT).[19] In this study, we considered an isolated infinite chain of polyimides. The true dielectric permittivity of the polymer chain alone was then extracted by combining the DFPT computation of the supercell, containing a significant amount of vacuum, with effective medium theory, using a recently developed method.[20]

3. RESULTS AND DISCUSSION

3.1. Initial Screening Using Density Functional Theory. The DFT-based quantum mechanical electronic structure method allows for the determination of atomic level interactions accurately, providing both the static (low-frequency) and optical (electronic) dielectric constant and the band gap for given configurations of atoms.[21,22] To identify promising structures, we used DFT computation in a high-throughput mode to conduct an initial combinatorial screening.[23] We considered an all-trans single polymer chain containing four independent blocks with periodic boundary conditions along the chain axis, without interchain interactions

being considered. Each block was assigned as one of the following units: -CH_2-, -NH-, -C(=O)-, -C(=S)-, -O-, -C_6H_4- (benzene ring), and -C_4H_2S- (thiophene ring). Combination of these blocks yields different types of polymers, including polyimides, polyureas, polyurethanes, polyamides, etc., resulting in 267 unique and reasonable structures. Polymer structures with a total dielectric constant (electronic and ionic) of >4 and a band gap of >3 were selected as promising candidates, as shown in Figure 1. These polymers are found to be composed

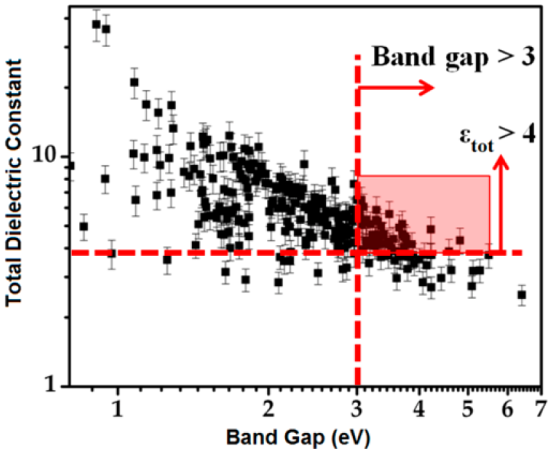

Figure 1. DFT-based initial screening results.

of aromatic group and polar blocks -NH-, -C(=O)-, and -O-. This work mainly focuses on the exploration of polyimide by combining various chain segments to tailor dielectric properties.

3.2. Synthesis and Basic Characterization of Polyimides. Polyimides were prepared by two-step polycondensation (Scheme 1),[24] with NMP as the solvent and isopropylamine as the end-capping reagent (2 mol % to the total of the anhydride group). Poly(amic acid) was formed at room temperature under an inert atmosphere followed by imidization at 170−180 °C. Syntheses of polyimides based on Jeffamines are described with the structure determination by FTIR, ^{1}H NMR, and GPC in the Supporting Information. Table 1 lists the thermal properties obtained by TGA and DSC. Polyimides with polyether segments have lower decomposition temperatures, because Jeffamine segments contain a methyl group and ether linkage that are more sensitive to thermal degradation.[25] They also exhibit a lower glass transition temperature (T_g). Only polyimides **B1** and **B2** were found to be semicrystalline. Compared to polypropylene, with a low T_g of 0 °C but high crystallinity, most of the polyimides here are amorphous, which requires a T_g higher than the operation temperature.

3.3. Polyimide Film Preparation. The incorporation of a polyether segment improves the solubility of polyimides. Polyimides based on Jeffamines are soluble in THF, DMF, DMAc, DMSO, NMP, and *m*-cresol at room temperature, making solution casting feasible. Films were prepared by casting 10 wt % THF solutions onto stainless steel shim stocks and drying them *in vacuo* at 40 °C for 10 h and then at 150 °C for 10 h. Polyimides **B1** and **B2** dissolve in only *m*-cresol at room temperature. For these polyimides, 10 wt % *m*-cresol solutions were used for casting and further drying at 150 °C for 10 h. Polyimide films prepared by the method described above were used for dielectric spectroscopy and band gap determination.

Large scale films were made by casting on a glass plate followed by the same drying process for breakdown strength measurement. **B2** was found to possess the best film forming quality, with large scale films made by using a 3 in. wide Dr. Blade coater. The blade gap was set to 356 μm. Drying of these films was performed using a real-time measurement system,[26] which monitors the weight, thickness, and in-plane and out-of-plane birefringence to track physical changes in the film during drying. The temperature and the air flow inside a real-time measurement system were set to 70 °C and 3 m/s, respectively. The film was soaked overnight in a water bath for ease of peeling from the glass substrate. The dried films were then used for breakdown strength measurement.

3.4. Dielectric Properties of Polyimides. Dielectric properties of polyimides were evaluated by the dielectric constant, dissipation factor (tan δ), and their variations with frequency and temperature, as well as band gap and breakdown strength.

3.4.1. Dielectric Constant and Loss. The dielectric constants (room temperature, 1 kHz) of the synthesized polyimides are listed in Table 2. All the polyimides have dielectric constants higher than that of BOPP because of the orientational polarizability of the imide functional group. Higher dielectric constants were achieved compared to those of common commercial polar polymers, including poly(ether imide) (PEI, dielectric constant of 3.2, dissipation factor of 0.21%), poly(phenylene sulfide) (PPS, dielectric constant of 3.1, dissipation factor of 0.30%), and poly(ether ether ketone) (PEEK, dielectric constant of 3.1, dissipation factor of 0.18%) tested at room temperature and 1 kHz.[5] The highest value achieved is 7.8 for **B4**. Incorporation of the polyether segment enhances the orientational polarizability and, hence, increases the dielectric constant further, as established by polyimides derived from Jeffamines having dielectric constant higher than those derived from diaminopropane and diaminohexane. Similarly, Jeffamine HK511 resulted in higher dielectric constants versus Jeffamine D230. Although side groups on the polymer backbone may possess higher mobility, they increase the free volume of the polymer chain, resulting in a lower density of dipole moments.

In addition, the dielectric constant was found to be greatly dependent on the bridge of the dianhydride structure. Via comparison of **B3** and **C3** to **A3**, a benzophenone or diphenyl ether structure leads to higher dielectric constants as additional dipole moments. However, unlike a carbonyl bridge in the

Table 1. Thermal Properties of Polyimides

	B1	B2	A3	A4	B3	B4	C3	C4	D3	D4
$T_g{}^a$ (°C)	174	150	75	53	82	78	72	63	98	81
$T_m{}^b$ (°C)	271	234	N/O	N/O	N/O	N/O	N/O	N/O	N/O	N/O
$T_o{}^c$ (°C)	350	338	333	313	325	317	354	341	324	283
$T_d{}^d$ (°C)	498	482	458	450	452	447	465	461	453	452

[a]Measured at the midpoint of the transition. [b]Melting temperature. [c]Onset temperature of degradation. [d]Maximal derivative of weight loss.

Table 2. Dielectric Properties (room temperature) of Polyimides

	B1	B2	A3	A4	B3	B4	C3	C4	D3	D4
$\varepsilon_{1\ kHz}$	4.01	3.57	4.17	5.44	4.52	7.80	4.37	6.04	2.50	5.26
tan $\delta_{1\ kHz} \times 100$	0.255	0.849	0.518	0.660	0.256	0.555	0.166	0.714	1.47	0.791
E_g (eV)	3.79	3.42	3.48	3.39	3.50	3.48	3.62	3.58	3.98	3.93

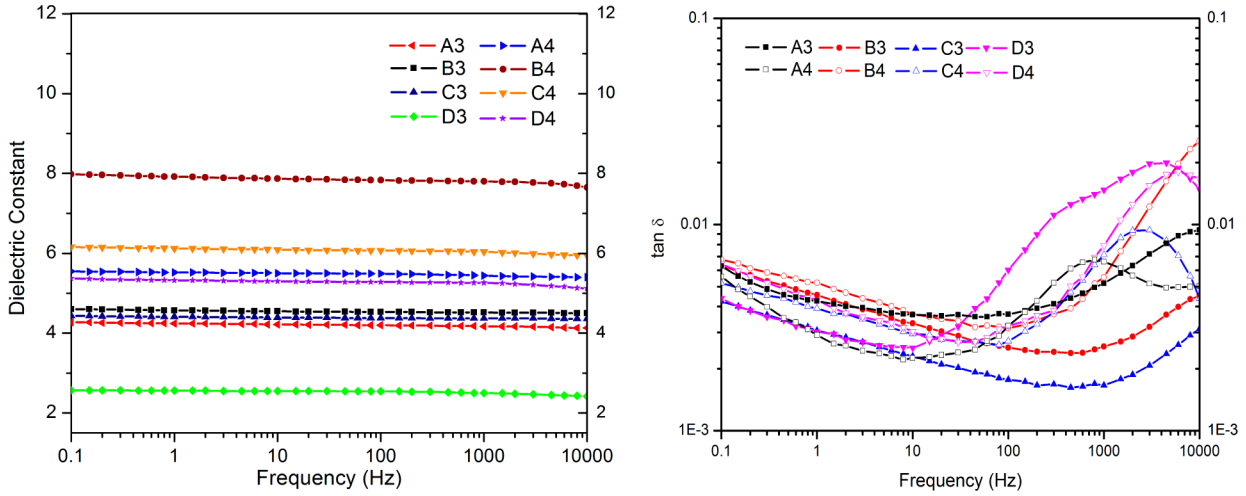

Figure 2. Dielectric constant (left) and loss (right) vs frequency at room temperature.

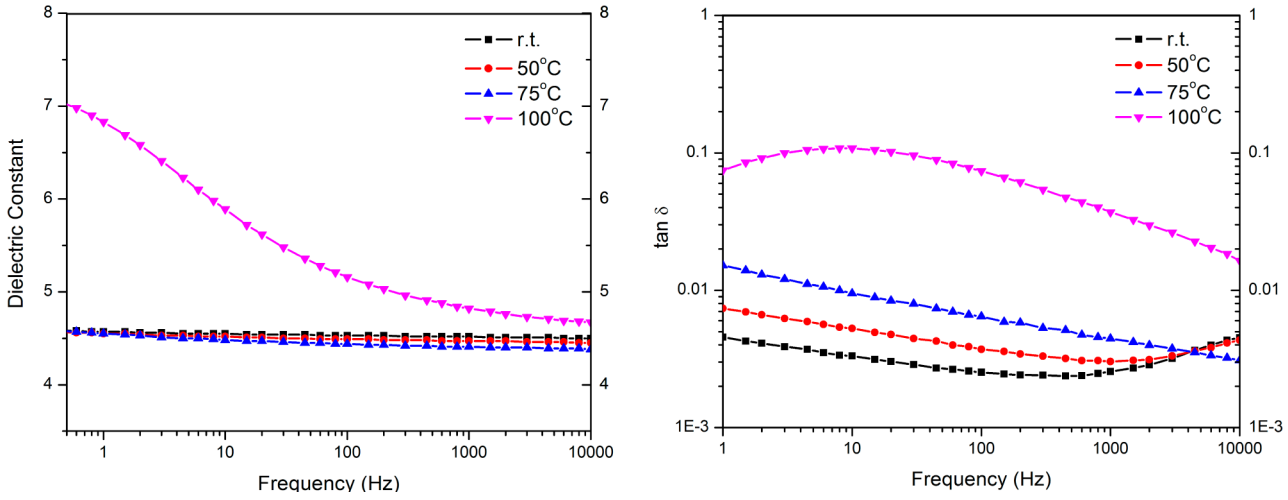

Figure 3. Dielectric constant (left) and tan δ (right) of polyimide B3 at different temperatures.

benzophenone structure, an ether linkage in diphenyl ether breaks the cross conjugation between two benzene rings, meaning limited delocalization and a lower mobility of π-electrons. Therefore, the benzophenone structure exhibits a polarizability higher than that of the diphenyl ether. Among all the polyimides, **B4**, having the longest cross-conjugated system as well as the longest polyether segment, exhibits the highest dielectric constant among all the samples. **D3** shows a much lower dielectric constant, because of the bulky trifluoromethyl group that weakens interchain electronic interactions, resulting in less efficient molecular packing.[27]

The dissipation factors of polyimides studied here all remain below 1% at room temperature and 1 kHz, with the exception of that of **D3**. Although there is relaxation behavior in the power frequency range between 10^{-3} and 10^{3} Hz,[6] the dissipation factors remain below 3%, comparable to the values for other polar polymers studied recently for energy storage applications.[3,28−31]

3.4.2. Frequency and Temperature Dependence of the Dielectric Constant and Loss. Dielectric constants of polyimides (Figure 2, left) decrease with an increasing frequency, because the dipoles cannot orient fast enough to keep up with the alternating electric field. The dielectric constant is dependent on electronic, atomic, and orientational polarizations, with orientational polarization being much slower than the other two. When the frequency increases, the orientational polarization decreases, resulting in a slight decrease in the dielectric constant.

As shown in Figure 2 (right), the dissipation factor changes for each polyimide with an increasing frequency because of relaxation peaks. Polyimides based on Jeffamine HK511 show dissipation factors higher than those based on Jeffamine D230 and exhibit relaxation at lower frequencies.

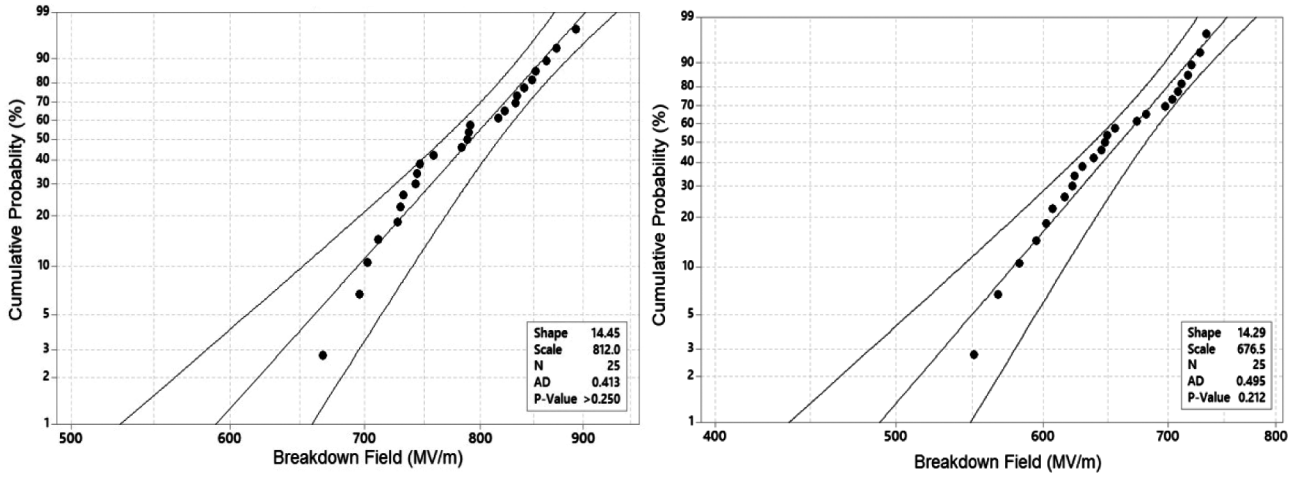

Figure 4. Weibull distribution of the breakdown field of **B2** (left) and **B4** (right) at room temperature.

The temperature dependence of the dielectric constant and loss was investigated by TDDS also. Figure 3 shows TDDS for **B3** as an example, with spectra of the other polyimides shown in the Supporting Information. The dielectric constant remains steady below T_g, which is 82 °C for **B3**, and increases dramatically at 100 °C. For amorphous polar polymers used in power storage capacitors, breakdown strength decreases considerably above T_g.[6] Therefore, to increase the operation temperature, a high T_g is necessary. Via comparison of data at 50 and 75 °C to those at room temperature, there is a slight decrease in the dielectric constant. The variation is insignificant but may be attributed to the loss of water upon heating the films.[31] Figure 3 (right) shows the dissipation factor for **B3**. Tan δ is less than 1% over most of the frequency range and increases with an increase in temperature. By investigating the transition peaks of all polyimides (Supporting Information) and comparing them with literature values,[30,31] we defined the transition peaks on the right-hand side of the spectrum as β relaxation peaks, and they move to a higher frequency when the temperature increases. At temperatures above T_g, a potential α relaxation develops at ~8 Hz.

3.4.3. Breakdown Strength and Band Gap. For an insulating material without defects and impurities, its intrinsic breakdown field should be a fixed value. As a result of impact ionization when electric stress is applied, electrons in the conduction band may transfer to the valence band to create an avalanche of electrons at breakdown fields, so the energy band gap indicates the breakdown strength. Band gap values obtained from UV absorption are listed in Table 2, where polyimides **D3** and **D4** possess the highest values followed by **C3** and **C4**. The polyimide with a longer ether linkage showed a slightly lower band gap. As the conjugation structure change with a switch in the dianhydride segment, delocalization of electrons increases the band gap as the conjugation or cross-conjugation length decreases. Compared to polyimides studied here, polypropylene as an example of most linear polyolefins has a higher band gap of 7.0 eV, but a low dielectric constant as mentioned above. This negative relationship between the band gap and dielectric constant is well-known for inorganic solids and has also been observed for organic polymer systems.[32]

Intrinsic breakdown is believed to be dependent on band gap, and it is understandable intuitively, as a material with a larger band gap tends to exhibit a higher threshold for impact ionization. The quantitative relationship between the band gap and intrinsic breakdown field was investigated on the basis of measured maximal breakdown voltage, which can be regarded as the approximate value of the intrinsic breakdown.[33−35] A power law dependence was found as the intrinsic breakdown increases when the band gap increases. However, the relationship appears to differ for different materials.[36] For a polymer material, establishing the relationship between the intrinsic breakdown and band gap is more challenging. First, the intrinsic breakdown is required to be obtained from a "perfect" material without high-field aging. However, the "perfection" of polymer materials is difficult to achieve macroscopically, because they are often amorphous or semicrystalline. Therefore, using the measured maximal breakdown voltage as the intrinsic breakdown is problematic. Second, the intrinsic breakdown is defined in terms of electron-avalanche theory, whereas the breakdown of the polymer usually depends on other mechanisms, including thermal breakdown, partial charge, and free volume breakdown. As for the polyimide, thermal breakdown is believed to be an important mechanism.[37]

The engineering dc breakdown was investigated in comparison with band gap values. The measurements were carefully conducted on free-standing films in silicone oil using ball bearing electrodes (diameter of $^1/_4$ in.). The Weibull distribution, which is based on the weak-link theory, is applied to characterize data.[38] The Weibull distribution function, $F(x)$, is given as

$$\begin{cases} F(x) = 1 - \exp\left[-\left(\dfrac{x-c}{\eta}\right)^{\beta}\right] & \text{for } x \geq c \\ F(x) = 0 & \text{for } x < c \end{cases}$$

where x is the electric field; η is the scale parameter, defined as the Weibull characteristic breakdown field here (the breakdown field at 63.2% probability); β is the shape parameter, which is a measure of dispersion in the data; and c is the threshold field below which no breakdown will occur. The two-parameter Weibull distribution is obtained when $c = 0$ and is employed here.

Measurements were conducted on **B2**, which possesses the best film forming quality, and **B4**, which exhibits the highest dielectric constant (Figure 4). The Weibull characteristic breakdown fields of **B2** and **B4** are 812 and 676 MV/m,

which results in potential energy densities of 9.98 and 15.77 J/cm^3, respectively. The Anderson-darling test parameter (critical value of 0.745 for 25 data points) for the fitting of **B4** is higher than that of **B2**. With a comparable band gap, the measured breakdown strength of **B2** is much higher than that of **B4**. These suggest that the film quality of **B4** needs to be improved by exploring different solvents and casting conditions, which affects the morphology and surface roughness of the films.[28] In addition, the measured breakdown field here indicates a possible extrinsic breakdown, which is not inherent to the material itself and is affected by chemical impurities, cavities, uniformity in microstructure, etc.

To confirm the structure−property relationship explored above, several polyimide structures similar to the ones synthesized were estimated by DFT calculations. Given the irregularity of the structure of the polyimides based on Jeffamines, the calculation time would be excessive. Therefore, we considered only several similar but more regular structures (Figure 5). It is obvious that polyimides V and VI have high

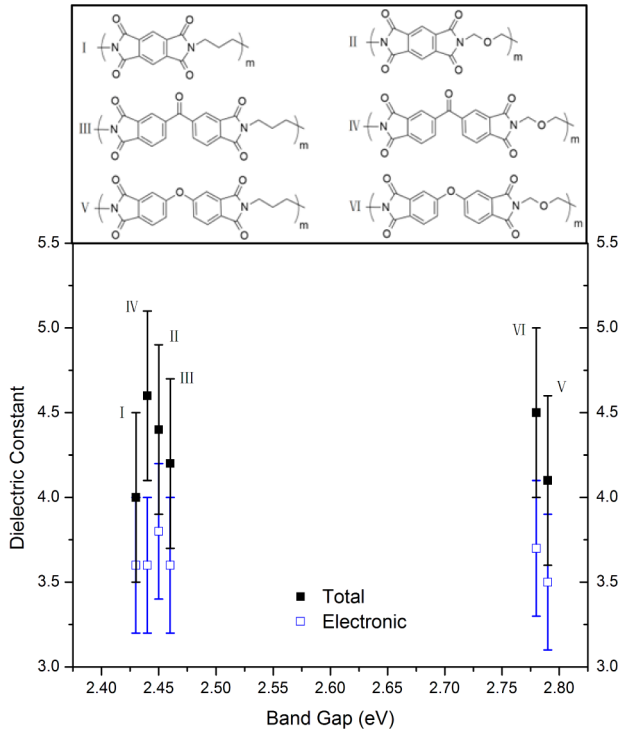

Figure 5. DFT calculation results for polyimides.

band gaps because of less conjugation, which matches the experimental results. However, the calculated values of the band gap are lower than the real values, because a well-known deficiency of the DFT approach is that under the local or semilocal approximations due to the self-interaction error, the lack of a long-range correlation effect, and the poor description of the electron−hole interaction in the excited states, DFT underestimates the energy band gap. For the dielectric constant, the addition of the ether linkage leads to a higher dielectric constant, matching the experimental results. The average value of the total dielectric constant of polyimide III is higher than that of I, indicating the benzophenone structure should give a higher dielectric constant, which applies for polyimides II and IV, as well. As for the precision of the calculated values of the dielectric constant and band gap, although the trend fits the experimental data, there is a difference between the two. The limitation of the calculations here is that we considered only single chains, without specification of polymer interchain interactions.

4. CONCLUSION

Through rational design, polyimides were determined to be a significant class of polymers for study as high-dielectric constant, low-loss materials for energy storage applications. The trends observed in the experimental results were corroborated by the DFT calculations. In this study, one of the highest dielectric constants of 7.8 for polyimide **B4** was achieved, with a potential energy density of ∼15 J/cm^3. This established the importance of the increased dipole volume from the ether linkage as well as the longer conjugation length when a carbonyl spacer was inserted between the benzene rings on the dielectric constant. The thermal limitation of **B4** can be solved through copolymerization with alkyl diamine, for example, diaminohexane to increase the operating temperature, which will be used in the future work. The band gap was used to predict the intrinsic breakdown voltage, with breakdown field measurements on **B4**. This work provided insights into polyether-containing polyimides as promising dielectric materials for achieving a high energy density.

■ ASSOCIATED CONTENT

Ⓢ Supporting Information

Synthesis and chemical structure determination of polyimides. This material is available free of charge via the Internet at http://pubs.acs.org.

■ AUTHOR INFORMATION

Corresponding Author

*E-mail: sotzing@mail.ims.uconn.edu.

Notes

The authors declare no competing financial interest.

■ ACKNOWLEDGMENTS

This work is supported by a multidisciplinary university research initiative (MURI) grant through the Office of Naval Research (N00014-10-1-0944). We acknowledge Dr. Steven Boggs and Dr. Yang Cao for valuable suggestions and JoAnne Ronzello for performing dielectric measurements.

■ REFERENCES

(1) Beach, F.; McNab, I. Present and Future Naval Applications for Pulsed Power. *IEEE Trans. Magn.* **2005**, *3* (12), 1−5.

(2) Ku, C.; Liepins, R. *Electrical Properties of Polymers: Chemical Principles*; Hanser Publishers: New York, 1987; Chapter 1, pp 22−36.

(3) Wang, Y.; Zhou, X.; Chen, Q.; Chu, B.; Zhang, Q. Recent Development of High Energy Density Polymers for Dielectric Capacitors. *IEEE Trans. Dielectr. Electr. Insul.* **2010**, *17*, 1036−1042.

(4) Barshaw, E. J.; White, J.; Chait, M. J.; Cornette, J. B.; Bustamante, J.; Folli, F.; Biltchick, D.; Borelli, G.; Picci, G.; Rabuffi, M. High Energy Density (HED) Biaxially-Oriented Poly-Propylene (BOPP) Capacitors for Pulse Power Applications. *IEEE Trans. Magn.* **2007**, *43* (1), 223−225.

(5) Ho, J.; Jow, T. R. *Characterization of High Temperature Polymer Thin Films for Power Conditioning Capacitors*; Army Research Laboratory: Adelphi, MD, 2009; ARL-TR-4880.

(6) Zhu, L.; Wang, Q. Novel Ferroelectric Polymers for High Energy Density and Low Loss Dielectrics. *Macromolecules* **2012**, *45*, 2937−2954.

(7) Guan, F.; Pan, J.; Wang, J.; Wang, Q.; Zhu, L. Crystal Orientation Effect on Electric Energy Storage in Poly(vinylidene fluoride-co-hexafluoropropylene) Copolymers. *Macromolecules* **2010**, *43*, 384−392.
(8) Zhang, Z. C.; Chung, T. C. Study of VDF/TrFE/CTFE Terpolymers for High Pulsed Capacitor with High Energy Density and Low Energy Loss. *Macromolecules* **2007**, *40*, 783−785.
(9) Chu, B. J.; Zhou, X.; Ren, K. L.; Neese, B.; Lin, M. R.; Wang, Q.; Bauer, F.; Zhang, Q. M. A Dielectric Polymer with High Electric Energy Density and Fast Discharge Speed. *Science* **2006**, *313*, 334−336.
(10) Pan, J.; Li, K.; Chuayprakong, S.; Hsu, T.; Wang, Q. High-Temperature Poly(Phthalazinone Ether Ketone) Thin Films for Dielectric Energy Storage. *ACS Appl. Mater. Interfaces* **2010**, *2*, 1286−1289.
(11) Venkatasubramanian, N.; Wiacek, K. J.; Fries-Carr, S.; Fossum, E.; Dang, T. D. High-Temperature Polymer Dielectrics for Capacitive Energy-Storage Applications. *Polyimides Other High Temp. Polym.* **2007**, *4*, 393−406.
(12) Gonzalo, B.; Vilas, J. L.; Breczewski, T.; Pèrez-Jubindo, M. A.; De La Fuente, M. R.; Rodriguez, M.; Lèon, L. M. Synthesis, Characterization, and Thermal Properties of Piezoelectric Polyimides. *J. Polym. Sci., Part A: Polym. Chem.* **2009**, *47*, 722−730.
(13) Meador, M. A. B.; Wright, S.; Sandberg, A.; Nguyen, B. N.; Van Keuls, F. W.; Mueller, C. H.; Rodríguez-Solís, R.; Miranda, F. A. Low Dielectric Polyimide Aerogels as Substrates for Lightweight Patch Antennas. *ACS Appl. Mater. Interfaces* **2012**, *4*, 6346−6353.
(14) Miyagawa, T.; Fukushima, T.; Oyama, T.; Iijima, T.; Tomoi, M. Photosensitive Fluorinated Polyimides with a Low Dielectric Constant Based on Reaction Development Patterning. *J. Polym. Sci., Part A: Polym. Chem.* **2003**, *41*, 861−871.
(15) Shi, N.; Ramprasad, R. Atomic-scale Dielectric Permittivity Profiles in Slabs and Multilayers. *Phys. Rev. B: Condens. Matter Mater. Phys.* **2006**, *74*, 045318/1−045318/7.
(16) Perdew, J. P.; Burke, K.; Ernzerhof, M. Generalized Gradient Approximation Made Simple. *Phys. Rev. Lett.* **1996**, *77*, 3865−3868.
(17) Blochl, P. E. Projector Augmented-Wave Method. *Phys. Rev. B: Condens. Matter Mater. Phys.* **1994**, *50* (24), 17953−17979.
(18) Kresse, G.; Joubert, D. Projector Augmented-wave Method. *Phys. Rev. B: Condens. Matter Mater. Phys.* **1999**, *59* (3), 1758−1775.
(19) Baroni, S.; de Gironcoli, S.; Dal Corso, A. Phonons and Related Crystal Properties from Density-Functional Perturbation Theory. *Rev. Mod. Phys.* **2001**, *73*, 515−562.
(20) Pilania, G.; Ramprasad, R. Dielectric Permittivity of Ultrathin $PbTiO_3$ Nanowires from First Principles. *J. Mater. Sci.* **2012**, *47*, 7580−7586.
(21) Kresse, G.; Furthmuller, J. Efficient Iterative Schemes for Ab Initio Total-Energy Calculations Using A Plane-Wave Basis Set. *Phys. Rev. B: Condens. Matter Mater. Phys.* **1996**, *54*, 11169−11186.
(22) Shi, N.; Ramprasad, R. Local Properties at Interfaces in Nanodielectrics: An Ab Initio Computational Study. *IEEE Trans. Dielectr. Electr. Insul.* **2008**, *15*, 170−177.
(23) Wang, C. C.; Pilania, G.; Boggs, S. A.; Kumar, S.; Breneman, C.; Ramprasad, R. Computational strategies for polymer dielectrics design. *Polymer* **2014**, *55*, 979−988.
(24) Koning, C.; Teuwen, L.; Meijer, E. W.; Moonen, J. Synthesis and Properties of α,ω-Diaminoalkane Based Polyimides. *Polymer* **1994**, *35*, 4889−4895.
(25) Hsiao, S. H.; Yang, C. P.; Chu, K. Y. Synthesis and Properties of Poly(ether imide)s Having Ortho-Linked Aromatic Units in the Main Chain. *Macromolecules* **1997**, *30* (2), 165−170.
(26) Unsal, E.; Drum, J.; Yucel, O.; Nugay, I. I.; Yalcin, B.; Cakmak, M. Real-time Measurement System for Tracking Birefringence, Weight, Thickness, and Surface Temperature During Drying of Solution Cast Coatings and Films. *Rev. Sci. Instrum.* **2012**, *83*, 025114/1−025114/10.
(27) Kapton Polyimide Film: Summary of Properties; Polymer Products Department, Industrial Films Division, Du Pont Co.: Wilmington, DE, 1989.
(28) MacDonald, J. R.; Schneider, M. A.; Ennis, J. B.; MacDougall, F. W.; Yang, X. H. High Energy Density Capacitors. *Proceedings of the IEEE Electrical Conference*, Montreal, October 22−23; IEEE: New York, 2009; pp 306−309.
(29) Wu, S.; Li, W.; Lin, M.; Burlingame, Q.; Chen, Q.; Payzant, A.; Xiao, K.; Zhang, Q. M. Aromatic Polythiourea Dielectrics with Ultrahigh Breakdown Field Strength, Low Dielectric Loss, and High Electric Energy Density. *Adv. Mater.* **2013**, *25*, 1734−1738.
(30) Jacobs, J. D.; Arlen, M. J.; Wang, D. H.; Ounaies, Z.; Berry, R.; Tan, L. S.; Garrett, P. H.; Vaia, R. A. Dielectric characteristics of polyimide CP2. *Polymer* **2010**, *51*, 3139−3146.
(31) Chisca, S.; Musteata, V. E.; Sava, I.; Bruma, M. Dielectric Behavior of Some Aromatic Polyimide Films. *Eur. Polym. J.* **2011**, *47*, 1186−1197.
(32) Ohki, Y.; Fuse, N.; Arai, T. Band Gap Energies and Localized States in Several Insulating Polymers Estimated by Optical Measurements. *IEEE Conf. Electr. Insul. Dielectr. Phenom.* **2010**, 660−663.
(33) Vijh, A. K. Correlation between the Magnitudes of Dielectric Breakdown Fields in Alkali Halides and Their Lattice Constants. *J. Mater. Sci.* **1974**, *9*, 2052−2053.
(34) Couchman, P. R.; Proto, G. R.; Reynolds, C. L. Concerning the Correlation between Dielectric Breakdown Field Strength and Lattice Constant in Alkali Halides. *J. Mater. Sci.* **1976**, *11*, 576−577.
(35) Wang, L. Relationship between Intrinsic Breakdown Field and Bandgap of Materials. *IEEE 25th International Conference on Microelectronics*; IEEE: New York, 2006; pp 14−17.
(36) Sun, Y.; Bealing, C.; Boggs, S. A.; Ramprasad, R. 50+ Years of Intrinsic Breakdown. *IEEE Electrical Insulation Magazine* **2013**, *29*, 8−15.
(37) Ku, C.; Liepins, R. *Electrical Properties of Polymers: Chemical principles*; Hanser Publishers: New York, 1987; Chapter 4, pp 150−151.
(38) Dissado, L. A.; Fothergill, J. C. *Electrical Degradation and Breakdown in Polymers*; Peter Peregrinus Ltd.: London, 1992; Chapter 14, pp 433−440.